
X-Factor: Quality Is a Dataset-Intrinsic Property

Josiah Couch¹ Miao Li¹ Rima Arnaout^{2,3,4} Ramy Arnaout^{1,5,6}

¹Department of Pathology, BIDMC ²Department of Medicine, UCSF

³Bakar Institute for Computational Health Sciences, UCSF ⁴Center for Intelligent Imaging, UCSF

⁵Division of Clinical Informatics, BIDMC ⁶Harvard Medical School

{jcouch1,mli22,rarnaout}@bidmc.harvard.edu rima.arnaout@ucsf.edu

Abstract

In the universal quest to optimize machine-learning classifiers, three factors—model architecture, dataset size, and class balance—have been shown to influence test-time performance but do not fully account for it. Previously, evidence was presented for an additional factor that can be referred to as dataset quality, but it was unclear whether this was actually a joint property of the dataset and the model architecture, or an intrinsic property of the dataset itself. If quality is truly dataset-intrinsic and independent of model architecture, dataset size, and class balance, then the same datasets should perform better (or worse) regardless of these other factors. To test this hypothesis, here we create thousands of datasets, each controlled for size and class balance, and use them to train classifiers with a wide range of architectures, from random forests and support-vector machines to deep networks. We find that classifier performance correlates strongly by subset across architectures ($R^2 = 0.79$), supporting quality as an intrinsic property of datasets independent of dataset size and class balance and of model architecture. Digging deeper, we find that dataset quality appears to be an emergent property of something more fundamental: the quality of datasets’ constituent classes. Thus, quality joins size, class balance, and model architecture as an independent correlate of performance and a separate target for optimizing machine-learning-based classification.

1 Introduction

Since the initial observation that neural-network models obey certain scaling laws [1], there have been many empirical [2, 3, 4, 5, 6] and theoretical [7, 8, 9, 10, 11, 12, 13, 14, 15, 16] studies examining the effects of training-set size and class balance (measured as the entropy of the class frequencies), model complexity (measured as the number of parameters in the model), and training effort (measured as amount of compute) on performance (measured as error or accuracy). However, these factors do not fully account for the variance in performance observed among models trained on different training sets. It stands to reason that some additional feature of training sets should be involved that might reasonably be termed “quality.”

Consider the well-known (but possibly apocryphal) anecdote about a classifier trained to look for tanks [17]. The story goes that while the model achieved 100% test accuracy during training, it failed on real-world examples, because in the training set all the images with tanks also contained clouds and all the images without tanks lacked them. It is no surprise that a classifier trained on such a training set would perform poorly on real-world examples, regardless of how large or class-balanced the training set was, how complex the model was, or how long it was trained for. But does an X-factor that we might call training-set quality truly exist? And if so, are we sure that it is intrinsic to the training set, as opposed to being some joint property of the dataset and the model used for

classification? Here we address these questions, to explore and better define the notion of training-set quality.

A 2024 study [18] proposed that quality does exist as an intrinsic property of training sets, and specifically that it could be measured using an entropic quantity called the metacommunity alpha diversity, part of the similarity-aware-diversity framework referred to as LCR [19, 20, 21]. This diversity is interpreted as the effective number [21] of image-class (or image-label) pairs in the training set, after accounting for the pairwise similarities and differences among images. (The presence of similarity means that the *effective* number is never greater than the *actual* number.)

In LCR, diversity and entropy are related by exponentiation. That an entropic measure might be related to training-set quality is reasonable in the context of the tanks-and-clouds example. That dataset has two separate “labels:” one that is being learned—tank vs. no tank—and a second that is irrelevant to the classification task—clouds vs. no clouds. If the training-set images were labeled for both clouds and tanks, the maximum-possible Shannon entropy of their joint distribution would be 2 bits—an LCR diversity of $2^2 = 4$ classes. This would be achieved by balancing a training set across all four combinations: tank/cloud, no-tank/cloud, tank/no-cloud, and no-tank/no-cloud. However, the entropy of the actual training set in the anecdote is only 1 bit (2 classes)—tank/cloud vs. no-tank/no-cloud—due to the (accidental) perfect correlation between these labels. This example makes it reasonable that training-set quality should be related to training-set entropy/diversity.

While that study did demonstrate a correlation between model performance and LCR’s metacommunity alpha diversity, the study only evaluated a single model architecture, ResNet-18 [18]. A more systematic test of whether quality is an intrinsic property of training sets requires comparing performance across multiple models. In addition, the subsets in the 2024 study were all constructed via random sampling (conditioned on maintaining maximal class balance). However, it is fair to expect that the performance will be similar for any subset created this way—i.e., that all random subsets are of similar quality, and that their performance will cluster tightly around the mean value—leaving not enough difference in performance to test the hypothesis.

To overcome these issues, it would be useful select for subsets in a way designed to bias the quality, as measured by model performance, away from this mean. Indeed, there is large amount of existing literature on various forms of subset selection spanning a variety of approaches, including active learning [22, 23, 24, 25, 26, 27, 28, 29, 30, 31, 32, 33], instance selection [34, 35, 36], dataset pruning [37, 38], and coreset selection [39, 40, 41, 42, 43, 44]. For example, a 2022 study [37] showed that the performance obtained by training on a random sampled subset can be improved upon by choosing either the “easiest” (for small datasets) or “hardest” (for large datasets) examples from a larger parent dataset. However, in this study easiest and hardest are defined with respect to a “probe” (i.e. weakly trained) perceptron classifier, which had to be trained prior to selection.

Here we use a subset-selection approach that avoids the need for pretraining by selecting images based on their root mean square differences (RMSDs). This approach is inspired by the LCR framework, in which the entropy/diversity of the dataset is a function of the elements’ pairwise similarities. Using this approach, we find that subsets’ performance indeed correlates strongly across model architectures, supporting the hypotheses that training sets do indeed possess intrinsic quality, irrespective of the model (or of size or class balance, which we control for).

2 Methods

2.1 Strategy (Fig. 1)

Using the MNIST handwritten digits dataset (Fig. 1a), we first generated random MNIST subsets of various sizes uniformly at random, but conditioned on their being perfectly class balanced, and characterized the performance of different models (see below) when trained on these subsets. Next, we generated additional class-balanced subsets of the same size, such that models trained on these subsets differed in performance from the uniformly random subsets (Fig. 1b). Finally, we tested whether differences in performance correlated across models (Fig. 1c-d), which definitionally demonstrated dataset-intrinsic correlation with performance irrespective of size or class balance, which we therefore referred to as training-set quality.

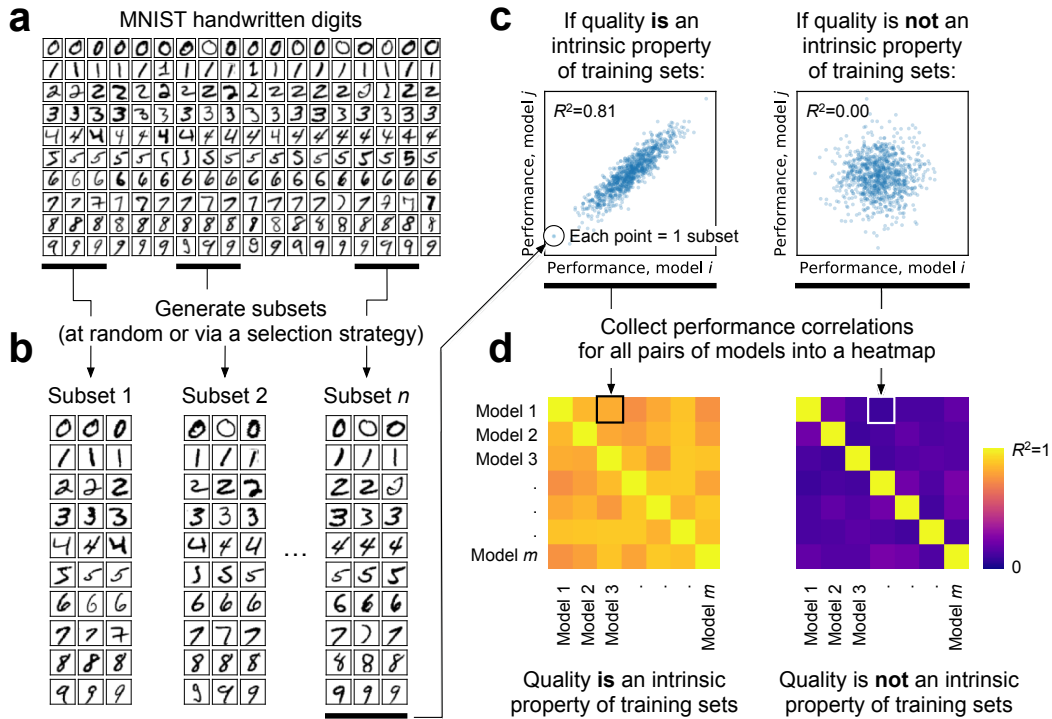


Figure 1: Schematic overview of research strategy. (a) Beginning with MNIST, (b) generate many subsets, either at random (“random subsets”) or according to one of several selection strategies (“selected subsets”), (c) compare how different models score these subsets, and (d) collect all correlations (e.g. into a heatmap). If performance is strongly correlated regardless of model—i.e. if the same subsets lead to the same relative performance for all model pairs—the conclusion is that this is because of some property intrinsic to training sets: a property that can be referred to as quality.

2.2 Models

We tested three classical architectures—random forest (RF), support-vector classifier (SVC), and Gaussian naive Bayes (GNB)—and five neural-network architectures—multilayer perceptrons (MLP) and ResNets (ResNet-18 and ResNet-34 [45]). Scikit-learn [46] was used for the classical models and pytorch [47] for the neural nets. The Appendix presents the details of how each model was run.

2.3 Datasets

All training sets were subsets of the 60,000 images in MNIST’s preselected training set of handwritten digits (which contains 6,000 images for each of the 10 digits 0-9 = 10 classes) (Fig. 1a) [48]. For a given fixed size of $n=10, 30, 100, 300,$ or 1000 images, we generated one group of subsets of size $10n$ by choosing n images of each digit uniformly at random. We refer to this baseline group as “random subsets.” We generated other groups (also of size $10n$) by oversampling $n + m$ ($m = 6, 10, 20, 30, 60, 100, 200, 300, 600,$ or 1000) images from each class and then selectively discarding the m excess images according to one of several selection strategies (below). We refer to these as “selected subsets.”

We performed positive and negative selection using each of four strategies, which we named “uniqueness”, “global mean”, “other mean”, “and own mean,” respectively (see Appendix). At each of our five sizes n , we selected 100 uniformly random subsets, and for each of the 10 choices of m , selection rule, and direction (positive vs. negative) we generated five selected subsets, leading to $4 \times 2 \times 10 \times 5 = 400$ selected subsets at each size. Factoring in the random subsets, the result was 500 total subsets at each size, and $500 \times 5 = 2,500$ subsets in total.

All selection strategies relied on the pixel-wise root-mean-square-difference (RMSD) distance between images. Three of these strategies calculated and made use of the mean training image per class, which for each class k was the 28×28 -pixel image that is the pixelwise mean of all the 6,000 images in the MNIST training set that belong to class k . Note that these selection strategies were not influenced by the content of the test set.

2.4 Training and testing

The training of the sklearn models (GNB, SVC, and RF) was performed using the default settings of `model.fit(X, y)`. Training of neural networks (ResNet-18, ResNet-34, and MLP-1 through 5) was done using cross-entropy loss and the Adam optimizer [49] with a batch size of 200 (note that for the smallest subsets, which had only 10 images per class, this results in only a partial batch per epoch). All models were trained for at least 50 epochs to a training set accuracy of 99%, or to a maximum of 500 epochs, whichever came first. The learning rate was initially set to $1e-3$, was reset to $1e-4$ on the second epoch, and was further reset to $1e-5$ if the 300th epoch was reached. All models trained on these subsets were tested against the predefined 10,000-image MNIST test set. Performance was assessed by the accuracy and the error ($= 1 - \text{accuracy}$). Note that because all training sets were class balanced, and the MNIST test set was also class balanced, accuracy and balanced accuracy are the same in this study.

2.5 Z-scores

We computed the mean and standard deviation of the error for training sets by subset size and for each model. We did this first for random subsets, as a baseline. We computed a Z-score for the error on each random subset by subtracting the relevant mean error and dividing by the relevant standard deviation. To compare selected subsets to random subsets, we then computed a Z-score for the error on each selected subset using the mean and standard deviation from the relevant random subsets (by size and model).

2.6 Correlations and confidence intervals

We computed R^2 (The square of Pearson’s R) of Z-scores for different models and (groups of) subsets. We bootstrapped the relevant set of subsets with 1,000 resamples to obtain 95% CIs on these R^2 s.

3 Results

We trained 10 different types of model on each of 2,500 MNIST subsets (Fig. 1). Three were classical (GNB, RF, and SVC) and seven were neural networks (five MLPs and two ResNets; see Methods). The 2,500 subsets consisted of 500 subsets at each of five different sizes: 100, 300, 1,000, 3,000, and 10,000

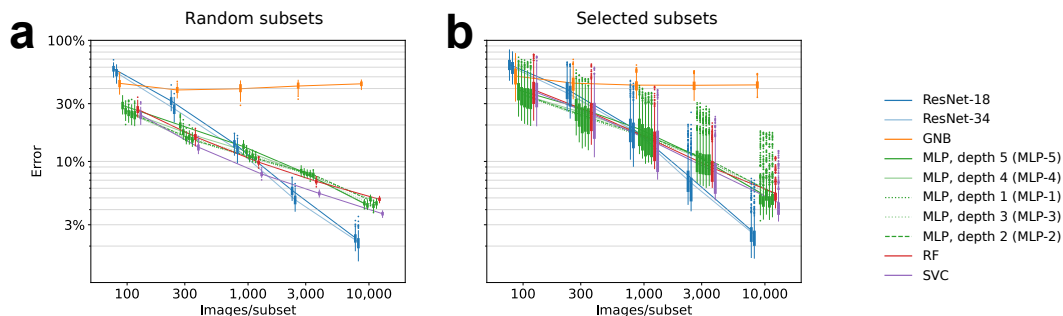


Figure 2: Performance of models on all (a) random and (b) selected subsets vs. subset size. The straight lines on these log-log plots demonstrate known scaling laws of performance with training-set size. Note the slopes are steeper for more expressive models. Importantly, performance on random subsets was tightly constrained compared to performance on selected subsets.

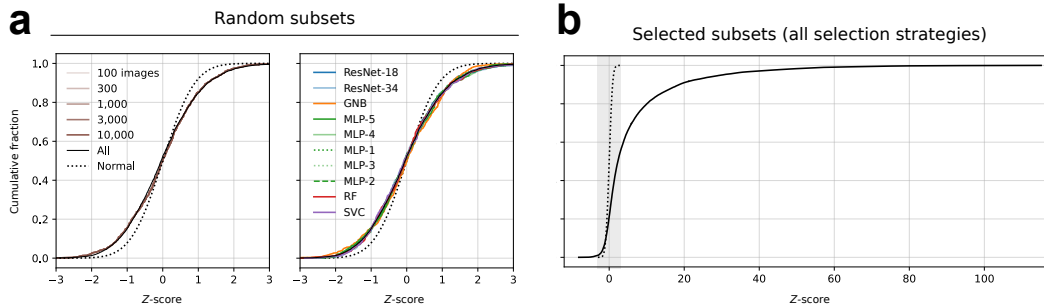


Figure 3: Scaled residual variance in performance from Fig. 2, plotted as cumulative density functions (CDFs) of Z-scores. (a) CDFs for random subsets pooled by subset size (left) and model (right) plotted against the CDF for a normal (Gaussian) distribution (dotted black line). Note their uniformity regardless of model or subset size, and how they differ subtly but reproducibly from the normal CDF (Kolmogorov-Smirnov $p < 10^{-5}$). Colors and linestyles are the same as in Fig. 2. (b) CDF for all selected subsets (solid black line) plotted against the CDF for a normal distribution (dotted black line). Note the much larger range of Z-scores for the selected subsets; the x-axis range for each of the plots in (a) is shown in gray in (b) for comparison.

10,000 images per subset, corresponding to 10, 30, 100, 300, and 1000 images per class for each of the 10 classes (Fig. 1a-b). Importantly, all subsets were perfectly class balanced, with the same numbers of images for each class. At each size, 100 of the subsets were generated by sampling images in each class uniformly at random (see Methods) and 400 were selected according to one of several selection strategies, to add different kinds of variation while maintaining maximal class balance. The motivation was that these “selected subsets” would show a wider variation in performance than class-balanced subsets generated by selecting images uniformly at random (“random subsets”), facilitating detection of trends that would support or falsify the hypothesis of quality as a dataset-intrinsic property.

Performance on random subsets varied by model and by subset size, recapitulating familiar log-log scaling laws with size, with steeper slopes for the more expressive models (Fig. 2a). The only exception to this pattern was GNB, which showed negligible trend with size, likely owing to its being too simple a model. Overall, error rates ranged from 1.5% to 70% by model and size. The classical models RF and SVC were the best performers on the smallest subsets, while the ResNets were the best performers on the largest. For subsets of a given size trained on a given model, performance clustered very tightly around the mean: model and subset size generally explained $>98\%$ of performance on the random subsets, leaving $<2\%$ residual variance.

In contrast, performance on the selected subsets ranged more widely for each subset size and model (Fig. 2b). Model and subset size together explained only 59-83% of the variance in performance on these subsets, leaving 17-41% residual variance unexplained (again excepting GNB). Interestingly, the selection strategies that generated the selected subsets only rarely led to better performance than obtained by the best random subsets. However, the goal was not better performance but simply a wider range of performance, to make any correlations across models easier to detect, and this goal was achieved.

The performance of random subsets clustered so tightly by size and model that we decided to examine them more closely. To compare these tight distributions to each other, we converted them from errors to Z-scores by subtracting off the mean error for each distribution—i.e. for each model and subset size—and then dividing the result by the standard deviation of that distribution. Surprisingly, we found the resulting distributions of residuals were indistinguishable from each other, regardless of model: they overlapped each other almost perfectly regardless of size (Fig. 3a) or model (Fig. 3b). One might expect these residuals to follow a normal (Gaussian) distribution; however, we found that they differed significantly from normal (Kolmogorov-Smirnov $p < 10^{-6}$), specifically in being slightly flattened. In contrast, the residual variance for the selected subsets was highly skewed (Fig. 3b). This pattern supports the conclusion that random subsets are in some fundamental sense all alike, but that outlier subsets with very different performance can be found using appropriate selection strategies.

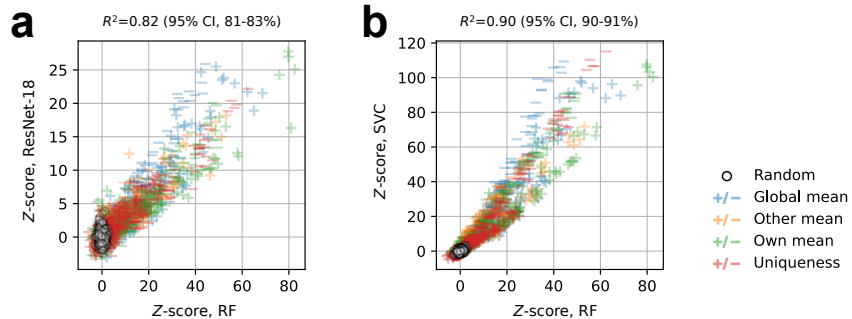


Figure 4: Training sets that perform better/worse by RF also tend to perform better/worse by (a) ResNet-18 and (b) SVC, two representative examples from among the 45 model pairs we compared. Colored + and - symbols, positively and negatively selected subsets, respectively. Note the random subsets cluster near Z-scores of zero, with only a few selected subsets outperforming them (corresponding to Z-scores below and to the left of them).

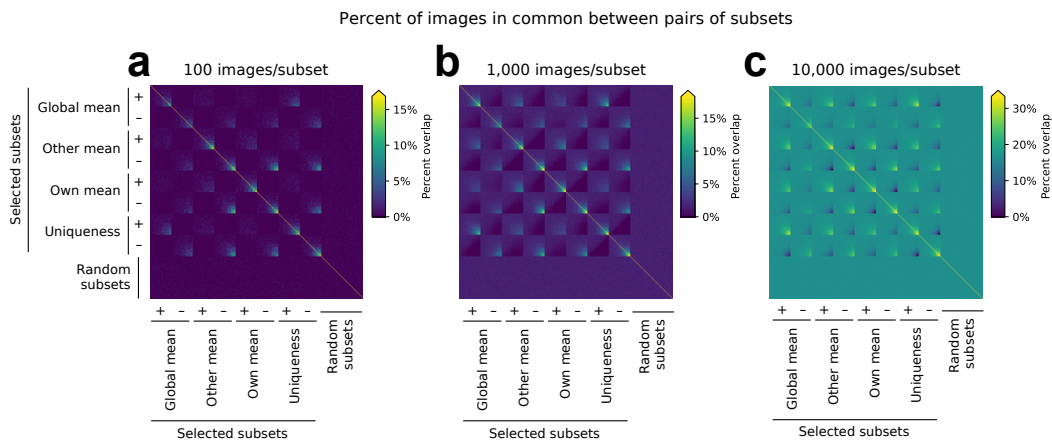


Figure 5: Percent of images that pairs of subsets have in common, for (a) 100, (b) 1,000, and (c) 10,000-image subsets. Positively selected subsets share images more than other pairs, yielding the faint checkerboard pattern. The color scale is saturated at the upper end to better visualize these effects.

Having demonstrated that our subsets exhibit a wide range of performance, as measured by error or Z-score, we next tested whether models performed better (or worse) on the same subsets. We did this by calculating Pearson’s correlation coefficient on the Z-scores for subsets according to each pair of models (Fig. 4). The resulting R^2 values (computed as the square of the Pearson’s correlation) were high, even between ResNets and traditional models such as RF and SVC. This was true regardless of subset size and selection strategy. The R^2 s were not due to selected subsets accidentally sharing a high percentage of images, as percent overlap between pairs of subsets was generally very low (Fig. 5). Fig. 6 collects the R^2 values for all pairs of models, illustrating the near-universality of this finding, supporting quality as an intrinsic property of datasets. Again, the only exception was GNB, which showed low R^2 with all other models. Given that GNB performance was always poor, with error rates of 32-83% (Fig. 2), and improved little if at all even as training-set size increased 100-fold, the likely explanation is that this model’s expressiveness is too limited to draw meaningful conclusions. Excluding it, we found the mean R^2 over all pairwise model comparisons was 0.82 (95% CI, 0.80-0.84). Thus, almost all of the residual variance in model performance was indeed explained by a property intrinsic to datasets, which can therefore be reasonably interpreted as quality.

Finally, we asked what the origin of this dataset-intrinsic quality property might be. Specifically, given that datasets are composed of classes, we asked whether or not performance on subsets’ classes might also correlate across models more than would be expected given the observed subset-level

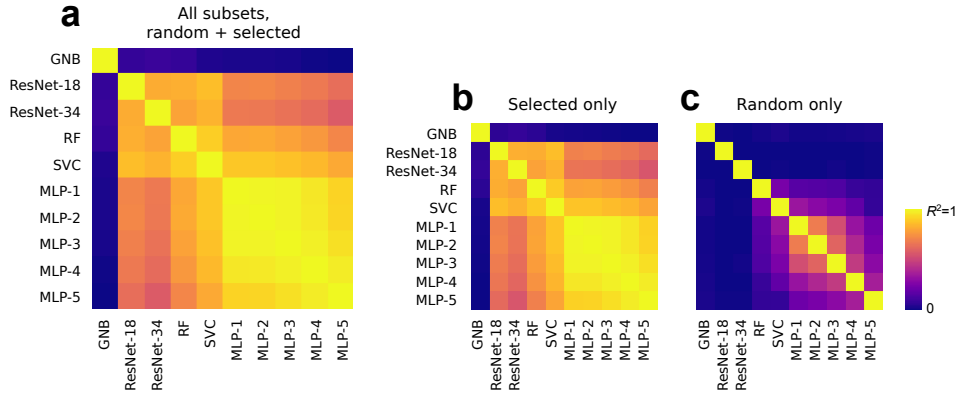


Figure 6: Performance correlations for all pairs of models for (a) all subsets, (b) selected subsets only, and (c) random subsets only. R^2 from comparisons such as those in Fig. 4 are shown. The pattern in (a) is driven by the selected subsets, explaining the similarity between (a) and (b). Note this pattern is largely absent from (c), consistent with our demonstration that random subsets exhibit very little variation in performance—too little to detect correlations across models—motivating the selection strategies that generated the selected subsets.

correlation. Indeed, we found almost universally high correlations for each class, i.e. for each of the digits 0-9, by Spearman’s ρ (Fig. 7). Further investigation is left for future work.

4 Discussion

Dataset generation and curation require significant time and energy, especially in technical and specialist areas such as medicine. Our results suggest that if a dataset results in especially high performance on model, it is more likely because of the dataset’s intrinsic quality than because of some idiosyncrasy of the model. This means that as new ML models are released, they are also likely to perform especially well on quality datasets, obviating the need to review the dataset for each new model, potentially saving substantial effort.

While the idea that datasets can be high or low quality is not new, the standard correlates of quality have simply been size and class balance. In contrast, here we demonstrate an intrinsic quality beyond those properties. While a 2024 study invoked this very phrase [18] to propose a reasonable entropic measure from the LCR framework as a way to quantify dataset quality, here we explicitly control for size and class balance and, by testing a variety of models, demonstrate that quality exists independent of those properties, is intrinsic to datasets, and seems to account for the large variance in residual model performance on training sets generated through the selection strategies we employed.

The wide variance in residual performance for selected subsets is in contrast to the very small variance in residual performance on random subsets, for which model architecture and training-set size explain nearly all the variance in performance as a whole through patterns consistent with known scaling laws. Not only do random subsets seem special in this respect, we demonstrated that the likelihood that they perform incrementally better or worse than expected seems to follow the same non-normal scaled distribution, the origin of which remains a mystery. Model-to-model stochasticity is a possibility for some models but not others; in any event, the extensive training procedure for the neural nets is expected to have minimized such variation in models that might be expected to be prone to it (deep nets).

The issue of residual variation arises also in Fig. 6a-b, which demonstrated that correlations in performance between models, while high (mean R^2 0.82), were not perfect. That figure also showed two blocks of substructure, in which the MLPs (perhaps not surprisingly) correlated very highly with each other in one block and the ResNets (more surprisingly) correlated very highly with RF and SVC in the other. Interestingly, this pattern was not obvious in the correlations in performance for the individual classes; there, if anything, RF and SVC correlated more strongly with the MLPs. While we largely ignore GNB as the highly non-expressive exception that proves the rule for most of our observations, we do note it correlates fairly well with most of the other models by class.

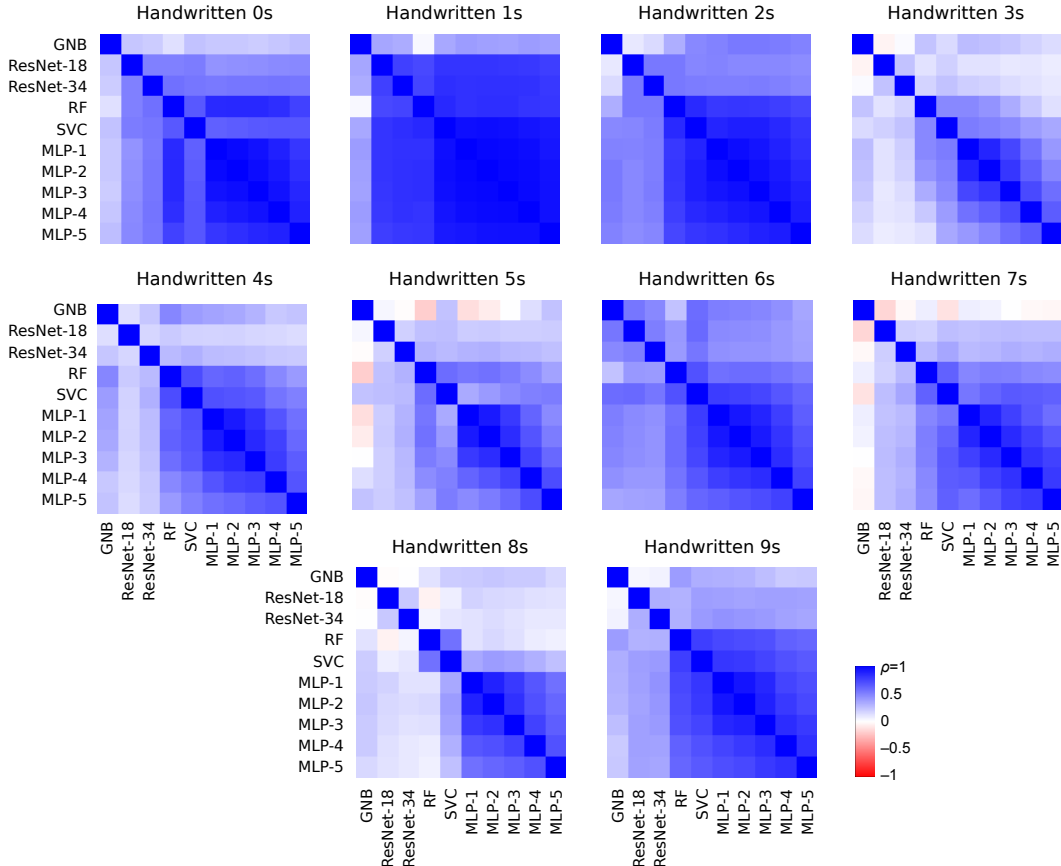


Figure 7: Spearman’s ρ for pairwise performance comparisons for each of the 10 classes in MNIST, across all subsets.

4.1 Limitations and Future Work

The sources and explanation for the correlations falling short of $R^2 = 1$ and for the variation in the patterns seen by class remain unanswered and suggest potentially interesting avenues for future work. In addition, the present work is limited by inclusion of only a single dataset (MNIST) and studying only classification tasks. Additional limitations are that while we have demonstrated that quality exists and that it is intrinsic to datasets (to an average R^2 of 0.82), we have not defined what quality is: i.e., we have not proposed or tested a quantitative measure of quality (such as the entropic measure proposed in [18]) or sought theoretical results. As a result, we cannot yet say what happens to quality when two high-quality subsets are combined: whether the quality of the subsets is additive vs. sub-additive (more likely) or whether they potentially even interfere with each other, resulting in lower quality in the combined set (which we consider unlikely but possible). Relatedly, investigation of how to optimize quality is left for future work.

Expanding this study to include larger training sets (by considering e.g. ImageNet as the source dataset) is conceptually straightforward. It is similarly straightforward, given a similarity metric between images, to compute LCR diversity indices (using e.g. [50]) or other measures of dataset entropy or diversity (such as the Vendi score from [51]) to determine whether or how well any of them might account for the correlations observed here. Both of these are left for future work.

A final limitation is the fact that the subset selection strategies we use largely only seem to hurt the performance of these models. Our conclusions would perhaps be more robust if we included more subsets that result in trained models with better performances than those trained on random subsets. This could perhaps be addressed by employing a selection strategy similar to what is employed in [37]. Our selection strategies were designed simply to increase the range of performances (which

they did) but not to improve performance (which they generally did not), and therefore should not be considered optimization strategies.

5 Conclusions

Overall, the conclusion from this study is that quality does exist as a property that is largely but not completely intrinsic to the training set and is independent of model architecture, dataset size, and dataset class balance. Thus, defining and optimizing dataset quality is expected to provide an independent mechanism for improving classifier performance for understanding at a more fundamental level what and how it is that models learn.

6 Support

This work was supported by the Gordon and Betty Moore Foundation and by the NIH under grants R01HL150394, R01HL150394-SI, R01AI148747, and R01AI148747-SI.

References

- [1] J. Hestness, S. Narang, N. Ardalani, G. Diamos, H. Jun, H. Kianinejad et al., *Deep learning scaling is predictable, empirically*, 1712.00409.
- [2] S. Ahmad and G. Tesauro, *Scaling and generalization in neural networks: A case study*, in *Advances in Neural Information Processing Systems*, D. Touretzky, ed., vol. 1, Morgan-Kaufmann, 1988, <https://api.semanticscholar.org/CorpusID:15615035>.
- [3] G. Prato, S. Guiroy, E. Caballero, I. Rish and S. Chandar, *Scaling laws for the few-shot adaptation of pre-trained image classifiers*, 2110.06990.
- [4] A. Althnain, D. AlSaeed, H. Al-Baity, A. Samha, A. B. Dris, N. Alzakari et al., *Impact of Dataset Size on Classification Performance: An Empirical Evaluation in the Medical Domain*, *Applied Sciences* **11** (2021) 796.
- [5] E. Caballero, K. Gupta, I. Rish and D. Krueger, *Broken neural scaling laws*, 2210.14891.
- [6] OpenAI, J. Achiam, S. Adler, S. Agarwal, L. Ahmad, I. Akkaya et al., *Gpt-4 technical report*, 2303.08774.
- [7] H. S. Seung, H. Sompolinsky and N. Tishby, *Statistical mechanics of learning from examples*, *Phys. Rev. A* **45** (1992) 6056.
- [8] Y. Bahri, E. Dyer, J. Kaplan, J. Lee and U. Sharma, *Explaining neural scaling laws*, *Proceedings of the National Academy of Sciences* **121** (2024) [2102.06701].
- [9] A. Maloney, D. A. Roberts and J. Sully, *A Solvable Model of Neural Scaling Laws*, 2210.16859.
- [10] E. J. Michaud, Z. Liu, U. Girit and M. Tegmark, *The quantization model of neural scaling*, 2303.13506.
- [11] H. Su, Z. Tian, X. Shen and X. Cai, *Unraveling the mystery of scaling laws: Part i*, 2403.06563.
- [12] Z. Zhang, *Neural Scaling Laws From Large-N Field Theory: Solvable Model Beyond the Ridgeless Limit*, 2405.19398.
- [13] B. Bordelon, A. Atanasov and C. Pehlevan, *A dynamical model of neural scaling laws*, 2402.01092.
- [14] A. Atanasov, J. A. Zavatone-Veth and C. Pehlevan, *Scaling and renormalization in high-dimensional regression*, 2405.00592.
- [15] N. Levi, *A simple model of inference scaling laws*, 2410.16377.
- [16] A. Brill, *Neural scaling laws rooted in the data distribution*, 2412.07942.
- [17] P. Riley, *Three pitfalls to avoid in machine learning*, *Nature* **572** (2019) 27.
- [18] J. Couch, R. Arnaout and R. Arnaout, *Beyond size and class balance: Alpha as a new dataset quality metric for deep learning*, 2407.15724.

- [19] T. Leinster and C. A. Cobbold, *Measuring diversity: the importance of species similarity*, *Ecology* **93** (2012) 477.
- [20] R. Reeve, T. Leinster, C. A. Cobbold, J. Thompson, N. Brummitt, S. N. Mitchell et al., *How to partition diversity*, 1404.6520.
- [21] T. Leinster, *Entropy and diversity: The axiomatic approach*, 2012.02113.
- [22] N. Houlsby, F. Huszár, Z. Ghahramani and M. Lengyel, *Bayesian Active Learning for Classification and Preference Learning*, 1112.5745.
- [23] Y. Gal, R. Islam and Z. Ghahramani, *Deep Bayesian Active Learning with Image Data*, 1703.02910.
- [24] P. Ren, Y. Xiao, X. Chang, P.-Y. Huang, Z. Li, B. B. Gupta et al., *A Survey of Deep Active Learning*, 2009.00236.
- [25] T. Kadota, H. Hayashi, R. Bise, K. Tanaka and S. Uchida, *Deep Bayesian Active-Learning-to-Rank for Endoscopic Image Data*, 2208.03020.
- [26] A. Kirsch, S. Farquhar, P. Atighehchian, A. Jesson, F. Branchaud-Charron and Y. Gal, *Stochastic Batch Acquisition for Deep Active Learning*, 2106.12059.
- [27] A. Kirsch and Y. Gal, *Unifying Approaches in Data Subset Selection via Fisher Information and Information-Theoretic Quantities*, 2208.00549.
- [28] S. Mindermann, J. Brauner, M. Razzak, M. Sharma, A. Kirsch, W. Xu et al., *Prioritized Training on Points that are Learnable, Worth Learning, and Not Yet Learnt*, 2206.07137.
- [29] A. Jesson, P. Tigas, J. van Amersfoort, A. Kirsch, U. Shalit and Y. Gal, *Causal-BALD: Deep Bayesian Active Learning of Outcomes to Infer Treatment-Effects from Observational Data*, 2111.02275.
- [30] Y. Huang, Y. Mabrouk, G. Gompper and B. Sabass, *Sparse inference and active learning of stochastic differential equations from data*, 2203.11010.
- [31] C. Riis, F. N. Antunes, F. B. Hüttel, C. L. Azevedo and F. C. Pereira, *Bayesian Active Learning with Fully Bayesian Gaussian Processes*, 2205.10186.
- [32] M. Ziatdinov, Y. Liu, K. Kelley, R. Vasudevan and S. V. Kalinin, *Bayesian Active Learning for Scanning Probe Microscopy: from Gaussian Processes to Hypothesis Learning*, 2205.15458.
- [33] M. Khosravani and S. Zilles, *Actively Learning Deep Neural Networks with Uncertainty Sampling Based on Sum-Product Networks*, 2206.09798.
- [34] E. Chinn, R. Arora, R. Arnaout and R. Arnaout, *Enrich: Exploiting image similarity to maximize efficient machine learning in medical imaging*, *Journal of the American Medical Informatics Association* **30** (2023) 1079 [medrxiv.org/content/10.1101/2021.05.22.21257645].
- [35] E. Chinn, R. Arora, R. Arnaout and R. Arnaout, *ENRICHing medical imaging training sets enables more efficient machine learning*, *Journal of the American Medical Informatics Association: JAMIA* **30** (2023) 1079.
- [36] T. Xie, J. Zhu, G. Ma, M. Lin, W. Chen, W. Yang et al., *Structural-Entropy-Based Sample Selection for Efficient and Effective Learning*, *arXiv e-prints* (2024) arXiv:2410.02268 [2410.02268].
- [37] B. Sorscher, R. Geirhos, S. Shekhar, S. Ganguli and A. S. Morcos, *Beyond neural scaling laws: beating power law scaling via data pruning*, *arXiv e-prints* (2022) arXiv:2206.14486 [2206.14486].
- [38] A. Maharana, P. Yadav and M. Bansal, *D2 Pruning: Message Passing for Balancing Diversity and Difficulty in Data Pruning*, *arXiv e-prints* (2023) arXiv:2310.07931 [2310.07931].
- [39] S. Har-Peled and A. Kushal, *Smaller Coresets for k -Median and k -Means Clustering*, *Discrete & Computational Geometry* **37** (2007) 3.
- [40] K. Killamsetty, X. Zhao, F. Chen and R. Iyer, *RETRIEVE: Coreset Selection for Efficient and Robust Semi-Supervised Learning*, 2106.07760.
- [41] C. Guo, B. Zhao and Y. Bai, *DeepCore: A Comprehensive Library for Coreset Selection in Deep Learning*, 2204.08499.

- [42] B. A. Griffin, J. Marks and J. J. Corso, *Zero-Shot Coreset Selection: Efficient Pruning for Unlabeled Data*, 2411 . 15349.
- [43] H. Chen, J. Peng, K. Tang, X. Geng and X. Yang, *Enhancing Multimodal In-Context Learning for Image Classification through Coreset Optimization*, 2504 . 14200.
- [44] H. Zheng, E. Tsai, Y. Lu, J. Sun, B. R. Bartoldson, B. Kailkhura et al., *ELFS: Label-Free Coreset Selection with Proxy Training Dynamics*, 2406 . 04273.
- [45] K. He, X. Zhang, S. Ren and J. Sun, *Deep residual learning for image recognition*, 1512 . 03385.
- [46] F. Pedregosa, G. Varoquaux, A. Gramfort, V. Michel, B. Thirion, O. Grisel et al., *Scikit-learn: Machine learning in Python*, *Journal of Machine Learning Research* **12** (2011) 2825.
- [47] A. Paszke, S. Gross, F. Massa, A. Lerer, J. Bradbury, G. Chanan et al., *Pytorch: An imperative style, high-performance deep learning library*, 1912 . 01703.
- [48] Y. LeCun, C. Cortes, C. Burges et al., *Mnist handwritten digit database*, 1998, .
- [49] D. P. Kingma and J. Ba, *Adam: A method for stochastic optimization*, 1412 . 6980.
- [50] P. Nguyen, R. Arora, E. D. Hill, J. Braun, A. Morgan, L. M. Quintana et al., *greylock: A python package for measuring the composition of complex datasets*, 2401 . 00102.
- [51] D. Friedman and A. Bousso Dieng, *The Vendi Score: A Diversity Evaluation Metric for Machine Learning*, *arXiv e-prints* (2022) arXiv:2210.02410 [2210 . 02410].
- [52] S. Marcel and Y. Rodriguez, *Torchvision the machine-vision package of torch*, in *Proceedings of the 18th ACM International Conference on Multimedia*, MM '10, (New York, NY, USA), p. 1485–1488, Association for Computing Machinery, 2010, DOI.

A Appendix

A.1 Model details

Random forest (RF)

The random forest classifier implementation from scikit-learn (`sklearn.ensemble.RandomForestClassifier`) is used with all default parameters, i.e.:

```
model = RandomForestClassifier()  
model.fit(X,y)
```

All scikit-learn models in this work are invoked this way.

Support-vector classifier (SVC)

We used scikit-learn’s (`sklearn.svm.SVC`) with default parameters.

Gaussian naive Bayes (GNB)

We used scikit-learn’s (`sklearn.naive_bayes.GaussianNB`) with default parameters.

Multilayer perceptrons (MLPs)

Using torch, we create MLPs of width `width` and depth `depth` with a single all-to-all input layer taking the `input_dim=28 × 28` input features and mapping them to a `width` dimensional space. This is followed by a ReLU activation function and `depth-1` additional all-to-all linear layers taking an input and output dimension of `width`, each followed by a ReLU. We then append a final all-to-all layer with input dimension `width` and output dimension 10 (the number of classes). We will refer to the `depth-1` through `depth-5` MLPs as MLP-1 through MLP-5.

Resnet

We start with the pre-trained resnets [45] available from torchvision [52] as `torchvision.models.resnet18` and `torchvision.models.resnet34`, both with default weights. We then overwrite the first (with `torch.nn.Conv2d`) and last (with `torch.nn.Linear`) layers of these models to correct for MNIST images being greyscale and having only 10 classes.

A.2 Selection strategies

a: Uniqueness

Positive selection eliminates images from each class that seem redundant (selection is for uniqueness). Negative selection keeps only the most redundant images.

For each class, beginning with $n + m$ images, positive selection first identifies the pair of images that has the smallest RMSD. For each image in this pair, the distance to its second nearest neighbor is computed. The image with the smallest distance is eliminated from the pair. This process repeats until only n images remain.

In negative selection, first the pair of images with the *largest* RMSD is identified. For each image in this pair, the distance to its second *furthest* neighbor is computed and the image with the *largest* distance is eliminated from the pair. Again, the process repeats, until only n images remain.

b: Global mean

For each class, this function first calculates the pixelwise mean image over all 6,000 images of that class in the MNIST training set, resulting in 10 mean images, one for each digit (i.e. one for each class). Then, for each of the subset’s $m + n$ images, we compute the RMSD between it and each of the 10 mean images. We then average these ten RMSD distances and associate this distance to the image. In positive selection, we keep the n images with the largest RMSD, maximizing distance from the global mean. In negative selection, we keep the n images with the smallest RMSD.

c: Other mean

This function starts with the same mean images as in *b*. For each class, for each image *i* in that class, we compute the RMSD to the mean image for each of the *other* classes. We take the maximum of these RMSDs and associate this value with image *i*. In positive selection, for each class we keep the *n* images with the highest values, the idea being to keep the images that in a sense “look least like” other digits. In negative selection, we keep the *n* images with the lowest values, i.e. those that look most like other digits.

d Own mean

This function also starts with the mean images in *b*. For each class, for each image in that class, we compute the RMSD to the mean image for *its own* class. In positive selection, we keep the *n* images with the smallest RMSD, i.e. the ones most like their own class mean; in negative selection, we keep the images with the largest RMSD, i.e. the ones least like their own class mean.

A.3 Hardware

All experiments were run on an Ubuntu workstation with an AMD Ryzen Threadripper PRO 7995WX 96-Cores CPU, 8 Samsung DIMM Synchronous Registered (Buffered) 5600 MHz (0.2 ns) memory cards, and two NVIDIA RTX 6000 Ada Generation graphics cards.

Generating the 500 uniformly random subsets took less than a second, and generating the 2000 selected subsets took around 161 minutes. Training the three classical models from sklearn took about an additional 64 minutes. The resnet-18 and resnet-34 models were re-trained in 244 and 393 minutes respectively. Finally, training the multi-layer perceptrons took between about 75 and 180 minutes each. Thus the entire pipeline took a bit longer than a day to run.

It should be noted that several variations of the current experimental pipeline were considered and run, and the results analyzed, prior to settling on the current version.

A.4 Assets and Licenses

MNIST dataset

This work makes use of the MNIST handwritten digits dataset [48]. The MNIST Dataset’s copyright is owned by Yann LeCun and Corinna Cortes, which is made available under the terms of the Creative Commons Attribution-Share Alike 3.0 license. More details in <http://www.pymvpa.org/datadb/mnist.html>. For the convenience of coding, we imported this dataset from PyTorch’s torchvision (license in a later section)

Models from sklearn

We used models from scikit-learn [46], including Random Forest, Support-vector classifier, and Gaussian naive Bayes. Scikit learn package is distributed under BSD 3-Clause License. More details <https://github.com/scikit-learn/scikit-learn?tab=BSD-3-Clause-1-ov-file>

Assets from torchvision

We used torchvision [52] for the MNIST dataset and resnet model with pretrained weights on ImageNet, all under the BSD 3-Clause License. More details at <https://github.com/pytorch/vision/blob/main/LICENSE>